Sensorless Indirect Field Oriented Control of Two-phase Induction Motor by Sliding Mode Flux/Speed Observer

Sam-Young Kim *, Seong-Su Park ** and Seung-Yub Park*
* Dept of Electronic Engineering, Changwon National University, Changwon, 641-773, Korea
Tel : +81-55-283-6353 Fax : +81-55-281-5070 E-mail: sam0kim, psy@changwon.ac.kr
**School of Mechatronics, Changwon National University, Changwon, 641-773, Korea
Tel : +81-55-279-8048 Fax : +81-55-281-5070 E-mail: sspark@changwon.ac.kr

Abstract: This paper investigated the speed sensorless indirect vector control of a two-phase induction motor to implement adjustable-speed drive for low-power applications. The sliding mode observer estimates rotor speed. The convergence of the nonlinear time-varying observer along with the asymptotic stability of the controller was analyzed. To define the control action which maintains the motion on the sliding manifold, an "equivalent control" concept was used. It was simulated and implemented on a sensorless indirect vector drive for 150W two-phase induction motor. The simulation and experimental results demonstrated effectiveness of the estimation method.

1. INTRODUCTION

The single-phase or two-phase induction motors have been widely employed in low or middle power level fields, especially in households where a three-phase supply is not available. At present, most of these applications, especially those with lower nominal power, utilize fixed-speed drives or conventional adjustable speed drives through voltage control using a triac or thyristors. Therefore, there is a great potential for energy savings if one manages to introduce energy efficient speed adjustable vector control into these areas on massive scale[1]-[2].

However, the problem lies in generally high cost for speed adjustable vector control compared to fixed or conventional adjustable speed drives, and difficulties in mounting the speed sensors due to environmental or mechanical restrictions.

In recent years, due to the advances in power electronic technology and low-cost high-performance digital signal processor, adjustable speed drives are being broadly applied. And a large amount of research effort has been spent in order to develop a reliable, low-cost control strategy for AC motor drives not needing speed sensors, called "sensorless" techniques. Numerous methods of sensorless vector control of induction motors are nowadays available. Magnetic-saliency-based[3]-[4], observer-based[5] and artificial intelligence(AI) based[6] sensorless methods have been proposed. But Most of these methods are applied to three-phase AC motor.

In this paper, the speed sensorless IFOC(indirect field-oriented control) of a two-phase induction motor is presented, based on a sliding mode rotor flux/speed observer in the two-phase stationary reference frame. The convergence of the nonlinear time-varying observer along with the asymptotic stability of the controller was analyzed. To define the control action which maintains the motion on the sliding manifold, an "equivalent control" concept was used[7]-[8].

The method has been implemented using the TMS320VC33 floating-point DSP controller. The performance and validity was proved by simulation and experiment on laboratory 150W two-phase induction motor drive system.

2. MODELLING AND IFOC METHOD OF THE TWO-PHASE INDUCTION MACHINE

The two-phase induction motor is composed of two symmetrical windings. That is, the number of windings of d-axis is the same as that of the windings of q-axis, and displaced 90 electrical degrees between these windings. Therefore, the mathematical model equations of two-phase induction motor may be equal to that of two-phase model of three-phase induction motor.

2.1. Stationary Reference Frame Model

A mathematical model of the two-phase may be described by the following set of ordinary differential equations in the stationary reference frame($\omega = 0$):

$$v_{ds}^s = R_s i_{ds}^s + p\lambda_{ds}^s \quad (1)$$

$$v_{qs}^s = R_s i_{qs}^s + p\lambda_{qs}^s \quad (2)$$

$$0 = R_r i_{dr}^s + p\lambda_{dr}^s + \omega_r \lambda_{qr}^s \quad (3)$$

$$0 = R_r i_{qr}^s + p\lambda_{qr}^s - \omega_r \lambda_{dr}^s \quad (4)$$

where, the stator and rotor flux linkage is described with the following equations (5)~(8):

$$\lambda_{ds}^s = L_s i_{ds}^s + L_m i_{dr}^s \quad (5)$$

$$\lambda_{qs}^s = L_s i_{qs}^s + L_m i_{qr}^s \quad (6)$$

$$\lambda_{dr}^s = L_r i_{dr}^s + L_m i_{ds}^s \quad (7)$$

$$\lambda_{qr}^s = L_r i_{qr}^s + L_m i_{qs}^s \quad (8)$$

where, R_s, R_r, L_s, L_r and L_m are the stator resistance, rotor resistance, stator inductance, rotor inductance and mutual inductance, respectively. Subscripts d and q denotes variables in the d,q-axis windings. Parameters and quantities with sub- or superscripts s and r are those in the stator and in the rotor, respectively. p denotes derivative operator. ω_r is rotor electrical angular velocity.

The instantaneous electromagnetic torque produced by the machine is then given by the equation:

$$T_e = P\frac{L_m}{L_r}(\lambda_{dr}^s i_{qs}^s - \lambda_{qr}^s i_{ds}^s) \quad (9)$$

where P is the number of pole pairs.

2.2. Synchronously Rotating Reference Frame Model

A mathematical model of the two-phase may be described by the following set of ordinary differential equations in the synchronously rotating reference frame($\omega = \omega_e$):

$$v_{ds}^e = R_s i_{ds}^e + p\lambda_{ds}^e - \omega_e \lambda_{qs}^e \quad (10)$$

$$v_{qs}^e = R_s i_{qs}^e + p\lambda_{qs}^e + \omega_e \lambda_{ds}^e \quad (11)$$

$$0 = R_r i_{dr}^e + p\lambda_{dr}^e - (\omega_e - \omega_r)\lambda_{qr}^e \quad (12)$$

$$0 = R_r i_{qr}^e + p\lambda_{qr}^e + (\omega_e - \omega_r)\lambda_{dr}^e \quad (13)$$

where the superscript e denotes synchronously rotating reference frame. The stator and rotor flux linkage is described with the following equations:

$$\lambda_{ds}^e = L_s i_{ds}^e + L_m i_{dr}^e \quad (14)$$

$$\lambda_{qs}^e = L_s i_{qs}^e + L_m i_{qr}^e \quad (15)$$

$$\lambda_{dr}^e = L_r i_{dr}^e + L_m i_{ds}^e \quad (16)$$

$$\lambda_{qr}^e = L_r i_{qs}^e + L_m i_{qs}^e \quad (17)$$

The electrical torque equation is

$$T_e = P\frac{L_m}{L_r}(\lambda_{dr}^e i_{qs}^e - \lambda_{qr}^e i_{ds}^e) \quad (18)$$

2.3. IFOC Method of Two-phase Induction Motor

From (16) and (18), d- and q-axis rotor currents in synchronous rotating frame are

$$i_{dr}^e = \frac{1}{L_r}(\lambda_{dr}^e - L_m i_{ds}^e) \quad (19)$$

$$i_{qr}^e = \frac{1}{L_r}(\lambda_{qr}^e - L_m i_{qs}^e) \quad (20)$$

Substituting (19) and (20) into (17) and (17) yields

$$p\lambda_{dr}^e + \frac{1}{T_r}\lambda_{dr}^e - \frac{L_m}{T_r} i_{ds}^e - \omega_{sl}\lambda_{qr}^e = 0 \quad (21)$$

$$p\lambda_{qr}^e + \frac{1}{T_r}\lambda_{qr}^e - \frac{L_m}{T_r} i_{qs}^e + \omega_{sl}\lambda_{dr}^e = 0 \quad (22)$$

where $\omega_{sl}(=\omega_e - \omega_r)$ is the slip angular speed. If the FOC is fulfilled such that q-axis rotor flux is zero and d-axis rotor flux is constant in synchronous rotating frame, the electromagnetic torque is controlled only by q-axis current from (18) and then

$$\lambda_{qr}^e = 0 \quad (23)$$

$$p\lambda_{qr}^e = 0 \quad (24)$$

$$p\lambda_{dr}^e = 0 \quad (25)$$

$$T_e = P\frac{L_m}{L_r}\lambda_{dr}^e i_{qs}^e \quad (26)$$

Substituting (23)-(25) into (12) and (20)-(22) yields

$$i_{dr}^e = 0 \quad (27)$$

$$i_{qr}^e = -\frac{L_m}{L_r} i_{qs}^e \quad (28)$$

$$\lambda_{dr}^e = L_m i_{ds}^e \quad (29)$$

$$\omega_{sl} = -\frac{R_r i_{qr}^e}{\lambda_{dr}^e} = -\frac{R_r i_{qr}^{e,*}}{\lambda_{dr}^{e,*}} = \frac{1}{T_r}\frac{i_{qs}^{e,*}}{i_{ds}^{e,*}} \quad (30)$$

where, the superscript * denotes the reference value.

The rotor flux angle is

$$\theta_e = \int (\omega_r + \omega_{sl})dt \quad (31)$$

3. THE PROPOSED FLUX/SPEED OBSERVER

3.1. Model-based Sliding Mode Observer

The model-based sensorless controller is a very popular method to estimate rotor speed using stator quantities. Specifically, only the stator currents and stator voltages are measured. A block diagram of the proposed model-based motor drive for sensorless IFOC of two-phase induction machine is shown in Fig. 1(a). A sliding mode based state observer is shown in Fig. 1(b).

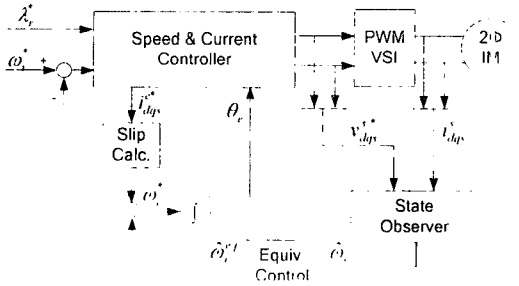

(a)

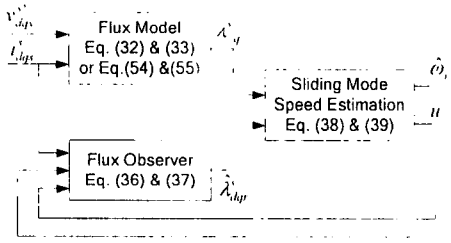

(b)

Fig. 1 (a) Schemetic of model-based senorless IFOC of two-phase induction motor. (b) Sliding mode based state observer

The proposed sliding mode state observer uses two independent observers to estimate the same quantities, the components of the rotor flux vector: one flux model (32) and (33) not involved ω_r derived from (1)-(4) and (5)-(8), and one sliding mode flux observer (36) and (37) involved ω_r based on (34) and (35).

Rotor flux observer not including ω_r terms are

$$p\lambda_{dr}^s = \frac{L_r}{L_m}[v_{ds}^s - (R_s + L_s\sigma p)i_{ds}^s] \quad (32)$$

$$p\lambda_{qr}^s = \frac{L_r}{L_m}[v_{qs}^s - (R_s + L_s\sigma p)i_{qs}^s] \quad (33)$$

Rotor flux observer including ω_r terms are

$$p\lambda_{dr}^s = \frac{L_m}{T_r} i_{ds}^s - \frac{1}{T_r}\lambda_{dr}^s - \omega_r \lambda_{qr}^s \quad (34)$$

$$p\lambda_{qr}^s = \frac{L_m}{T_r} i_{qs}^s - \frac{1}{T_r}\lambda_{qr}^s + \omega_r \lambda_{dr}^s \quad (35)$$

Applying the same structure of (34) and (35), the sliding mode rotor flux observer is proposed as

$$p\hat{\lambda}_{dr}^{s} = \frac{L_m}{T_r} i_{ds}^{s} - \frac{1}{T_r}\hat{\lambda}_{dr}^{s} - \hat{\omega}_r \hat{\lambda}_{qr}^{s} + u\hat{\lambda}_{qr}^{s} \quad (36)$$

$$p\hat{\lambda}_{qr}^{s} = \frac{L_m}{T_r} i_{qs}^{s} - \frac{1}{T_r}\hat{\lambda}_{qr}^{s} + \hat{\omega}_r \hat{\lambda}_{dr}^{s} - u\hat{\lambda}_{dr}^{s} \quad (37)$$

where continuous time function $\hat{\lambda}_{dr}^{s}$, $\hat{\lambda}_{qr}^{s}$ represent the estimated rotor flux, T_r is rotor time constant and σ is the motor leakage coefficient($\sigma = 1 - L_m^2/(L_s L_r)$). The estimate of angle speed $\hat{\omega}_r$ and auxiliary variable u are discontinuous parameters given by

$$\hat{\omega}_r = \omega_0 sign(s_\omega) \quad (38)$$

$$u = u_0 sign(s_u) \quad (39)$$

where $sign(s_{\omega u}) = \begin{cases} 1, & if \ s_{\omega u} > 0 \\ 0, & if \ s_{\omega u} = 0 \\ -1, & if \ s_{\omega u} < 0 \end{cases}$ and,

ω_0 and u_0 are positive constants. s_ω and s_u are nonlinear functions of rotor flux errors and estimated rotor flux.

$$s_\omega = (\hat{\lambda}_{dr}^{s} - \lambda_{dr}^{s})\hat{\lambda}_{qr}^{s} - (\hat{\lambda}_{qr}^{s} - \lambda_{qr}^{s})\hat{\lambda}_{dr}^{s} = \bar{\lambda}_{dr}^{s}\hat{\lambda}_{qr}^{s} - \bar{\lambda}_{qr}^{s}\hat{\lambda}_{dr}^{s} \quad (40)$$

$$s_u = (\hat{\lambda}_{dr}^{s} - \lambda_{dr}^{s})\hat{\lambda}_{dr}^{s} + (\hat{\lambda}_{qr}^{s} - \lambda_{qr}^{s})\hat{\lambda}_{qr}^{s} = \bar{\lambda}_{dr}^{s}\hat{\lambda}_{dr}^{s} + \bar{\lambda}_{qr}^{s}\hat{\lambda}_{qr}^{s} \quad (41)$$

3.2. Lyapunov Stability Analysis for the Proposed Observer

To analyze convergence of the estimates to the real values for the proposed rotor flux observer structure, the sliding mode observer equations with respect to the flux errors $\bar{\lambda}_{dr}^{s}$ (= $\hat{\lambda}_{dr}^{s} - \lambda_{dr}^{s}$) and $\bar{\lambda}_{qr}^{s}$ (= $\hat{\lambda}_{qr}^{s} - \lambda_{qr}^{s}$) can be written as

$$p\bar{\lambda}_{dr}^{s} = -\frac{1}{T_r}\bar{\lambda}_{dr}^{s} - \hat{\omega}_r \hat{\lambda}_{qr}^{s} + \omega_r \lambda_{qr}^{s} + u\hat{\lambda}_{qr}^{s} \quad (42)$$

$$p\bar{\lambda}_{qr}^{s} = -\frac{1}{T_r}\bar{\lambda}_{qr}^{s} + \hat{\omega}_r \hat{\lambda}_{dr}^{s} + \omega_r \lambda_{dr}^{s} - u\hat{\lambda}_{dr}^{s} \quad (43)$$

And Lyapunov's stability theorem gives a sufficient condition for asymptotic stability of a system by using a Lyapunov function[9]. Consider the following Lyapunov function V because the estimate of angle speed $\hat{\omega}_r$ and auxiliary variable u are function related to (40) and (41).

$$V = \frac{1}{2}s_\omega^2 + \frac{1}{2}s_u^2$$

The Lyapunov function V is positive definite. This satisfies the first Lyapunov stability condition. The second condition is that the derivative of the sliding mode function must be less than zero. i.e., $\dot{V} = s_\omega \dot{s}_\omega + s_u \dot{s}_u < 0$.

Using (36), (37) and (42), (43), $s_\omega \dot{s}_\omega$ yields

$$\dot{s}_\omega = \dot{\bar{\lambda}}_{dr}^{s}\hat{\lambda}_{qr}^{s} - \dot{\bar{\lambda}}_{qr}^{s}\hat{\lambda}_{dr}^{s} + \bar{\lambda}_{dr}^{s}\dot{\hat{\lambda}}_{qr}^{s} - \bar{\lambda}_{qr}^{s}\dot{\hat{\lambda}}_{dr}^{s} \quad (44)$$

$$\dot{\bar{\lambda}}_{dr}^{s}\hat{\lambda}_{qr}^{s} - \dot{\bar{\lambda}}_{qr}^{s}\hat{\lambda}_{dr}^{s} = -\omega_0 sign(s_\omega) \| \hat{\lambda} \|^2 - \frac{1}{T_r}s_\omega + \omega_r e_1 + u \| \hat{\lambda} \|^2$$

$$\bar{\lambda}_{dr}^{s}\dot{\hat{\lambda}}_{qr}^{s} - \bar{\lambda}_{qr}^{s}\dot{\hat{\lambda}}_{dr}^{s} = \omega_0 sign(s_\omega)s_u - \frac{1}{T_r}s_\omega - u \| \hat{\lambda} \|^2 + ue_1 - \frac{L_m}{T_r}e_2$$

And,

$$\dot{s}_\omega = -(\| \hat{\lambda} \|^2 - s_u)\omega_0 sign(s_\omega) - \frac{2}{T_r}s_\omega + f_\omega \quad (45)$$

Therefore,

$$s_\omega \dot{s}_\omega = -(\| \hat{\lambda} \|^2 - s_u)\omega_0 |s_\omega| - \frac{2}{T_r}s_\omega^2 + s_\omega f_\omega \quad (46)$$

Similarly, for $s_u \dot{s}_u$

$$s_u \dot{s}_u = s_u(\dot{\bar{\lambda}}_{dr}^{s}\hat{\lambda}_{dr}^{s} + \dot{\bar{\lambda}}_{qr}^{s}\hat{\lambda}_{qr}^{s} + \bar{\lambda}_{dr}^{s}\dot{\hat{\lambda}}_{dr}^{s} + \bar{\lambda}_{qr}^{s}\dot{\hat{\lambda}}_{qr}^{s})$$

$$= -\omega_0 |s_\omega| s_u + u_0 s_\omega |s_u| - \frac{2}{T_r}s_u^2 + s_u f_u \quad (47)$$

where, $\| \hat{\lambda} \| = \sqrt{\hat{\lambda}_{dr}^{s\,2} + \hat{\lambda}_{qr}^{s\,2}}$, $f_\omega = (\omega_r + u)e_1 - \frac{L_m}{T_r}e_2$,

$$f_u = \frac{L_m}{T_r}(i_{ds}^{s}\bar{\lambda}_{dr}^{s} + i_{qs}^{s}\bar{\lambda}_{qr}^{s}) - \omega_r(\lambda_{dr}^{s}\hat{\lambda}_{qr}^{s} - \lambda_{qr}^{s}\hat{\lambda}_{dr}^{s})$$

$$e_1 = \hat{\lambda}_{dr}^{s}\lambda_{dr}^{s} + \hat{\lambda}_{qr}^{s}\lambda_{qr}^{s} \quad (48)$$

$$e_2 = i_{ds}^{s}\bar{\lambda}_{qr}^{s} - i_{qs}^{s}\bar{\lambda}_{dr}^{s} \quad (49).$$

From (46) and (47)

$$\dot{V} = s_\omega \dot{s}_\omega + s_u \dot{s}_u \quad (50)$$

$$= -\| \hat{\lambda} \|^2 \omega_0 |s_\omega| + u_0 s_\omega |s_u| - \frac{2}{T_r}(s_\omega^2 + s_u^2) + s_\omega f_\omega + s_u f_u$$

$$= -[\| \hat{\lambda} \|^2 \omega_0 - u_0 |s_u| sign(s_w)] \ |s_\omega| - -\frac{2}{T_r}(s_\omega^2 + s_u^2) + s_\omega f_\omega + s_u f_u$$

It follows from (50) that, if the condition

$$u_0 << \omega_0 \quad (51)$$

is satisfied, then for high enough ω_0, $\dot{V} = s_\omega \dot{s}_\omega + s_u \dot{s}_u < 0$, i.e., sliding mode will occur on surface $s_\omega = 0$ and $s_u = 0$.

After sliding mode arises on the intersection of surface $s_\omega = 0$ and $s_u = 0$, then $\bar{\lambda}_{dr}^{s} = 0$ and $\bar{\lambda}_{qr}^{s} = 0$ under the assumption $\| \hat{\lambda} \|^2 \neq 0$, which means that the estimated flux $\hat{\lambda}_{dr}^{s}$, $\hat{\lambda}_{qr}^{s}$ converge to the real fluxes.

The sliding mode equations on $s_\omega = 0$ and $s_u = 0$ can be derived by replacing the discontinuous function $\omega_0 sign(s_\omega)$ and $u_0 sign(s_u)$ by the equivalent control value $\hat{\omega}_r^{eq}$ and u^{eq}, which are the solutions of the algebraic equations $\dot{s}_\omega = 0$. From (45), $\hat{\omega}_r^{eq}$ is

$$\hat{\omega}_r^{eq} = \frac{\omega_r}{\| \hat{\lambda} \|^2}e_1 - \frac{L_m}{T_r \| \hat{\lambda} \|^2}e_2 \quad (52)$$

If the estimated rotor flux converges to the real flux, the equivalent rotor speed will tend to the real speed. However, $\hat{\omega}_r^{eq}$ can not be calculated by the above equation, since it contains unknown real rotor fluxes in e_1 and e_2. In practice, the discontinuous control can be considered as a combination of an equivalent control term and a high frequency switching term. Therefore the equivalent control $\hat{\omega}_r^{eq}$ can be obtained through a low-pass filter with discontinuous value $\hat{\omega}_r$ as the input[7]-[8].

$$\hat{\omega}_r^{eq} \cong \frac{1}{\tau p + 1}\hat{\omega} \quad (53)$$

where the τ is the time constant of the filter. It should be sufficiently small to preserver the slow component undis-

torted but large enough to eliminate the high frequency components. The obtained equivalent control $\hat{\omega}_r^{eq}$ is used as feedback in the closed loop. In the paper, τ was selected as 0.0067. In case of higher value than this one, the closed loop system suffered from excessive speed ripple.

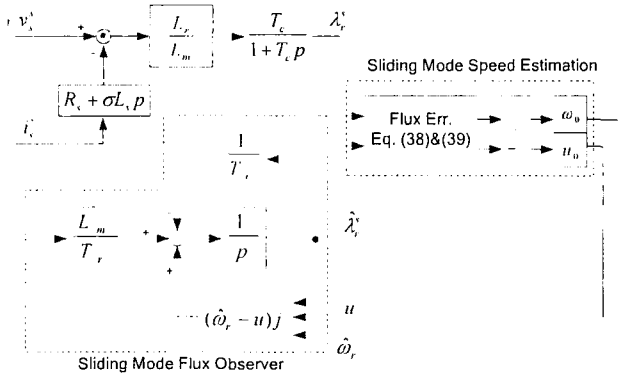

Fig. 2 Block Diagram of the proposed sliding mode flux/speed observer

3.4. Practical consideration of the sliding mode observer

In practice, the rotor flux by pure integration based on (32) and (33) can pose significant problems, particularly at low frequency, because of sensor noise, dc offset, and parameter detuning effect.

In this paper, to overcome these problems, 1'st high pass filter is applied to (32), (33). And then rotor flux is observed as follow

$$\lambda_{dr}^{s} = \frac{T_c}{1+T_c p}\frac{L_r}{L_m}[v_{ds}^{s} - (R_s + L_s\sigma p)i_{ds}^{s}] \qquad (54)$$

$$\lambda_{qr}^{s} = \frac{T_c}{1+T_c p}\frac{L_r}{L_m}[v_{qs}^{s} - (R_s + L_s\sigma p)i_{qs}^{s}] \qquad (55)$$

If the time constant T_c is small value, the influence of voltage and current offset is decreased. Against, if T_c is increased, phase error of the observed rotor flux is decreased. . In the paper, T_c was selected as 0.1. The block diagram of the proposed sliding mode flux/speed observer using flux observer (54) and (55) with high pass filter is shown in Fig. 2.

4. SIMULATION & EXPREMENTAL RESULT

4.1. Experimental System Configuration

Fig. 3 shows the sensorless IFOC configuration of two-phase induction motor using speed estimation algorithm by the proposed sliding mode observer. And Fig. 4 shows the system hardware configuration for experiment.

The speed and current controllers were implemented by PI controllers.

The current regulated four-switch voltage-fed inverter[10] and 150W two-phase induction motor was available for computer simulation and experimental study. The parameter of are given in Table 1.

The control system was implemented with the 32-bit digital processor TMS320VC33 operating with a clock frequency of 100 MHz and sampling interval is 125 μs for current control and speed estimation loop.

A sinusoidal PWM algorithm was used. Because the experimental target system is for a low power household appliance which seriously considered about energy efficiency, the PWM switching frequency of implemented system is 4 kHz with a dead time of 6μs considering the switching loss.

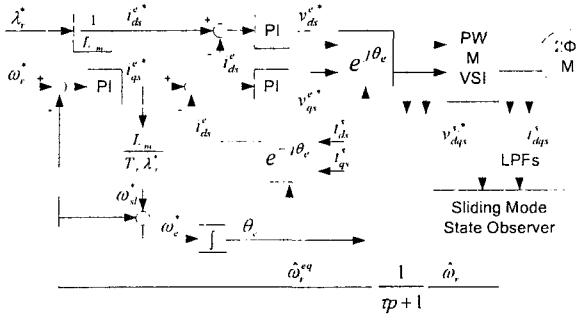

Fig.3 Schematic of the sensorless indirect vector drive system for two-phase induction motor

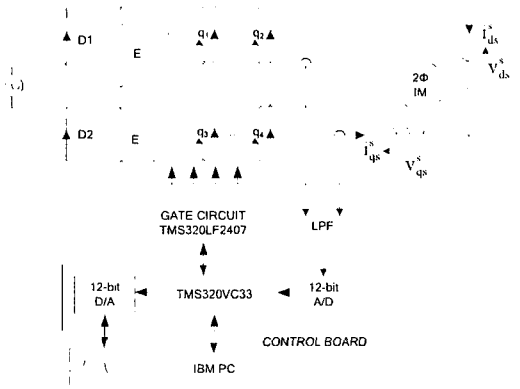

Fig.4 System hardware configuration.

Table 1 Parameter of Two-phase Induction Motor(75℃)

Rated output	150	[W]
Rated voltage	220	[V]
Rated main/aux winding current	1.63	[A]
Stator main/aux winding resistor	19.0	[Ω]
Rotor resistor	13.3	[Ω]
Main/aux winging inductance	34.7	[mH]
Rotor inductance	29.2	[mH]
Mutual inductance	371.4	[mH]
Pole	4	

4.2. Simulation Results

A detailed computer simulation was developed on MATLAB/SIMULINK. The validity of the proposed sliding mode flux/speed observer for speed sensorless IFOC of two-phase induction motor is verified by the simulation at trapezoidal reference(167.6 rad/s to -167.6 rad/s, ramp rate: ±41.9 rad/0.1sec) under no-load condition. The results are given in Fig. 5 and 6. In Fig. 6(b), observed speed error is less than 1.5[rad/s] at ramp range for speed transition. Fig. 6 shows the transition waveform at forward to reverse operation. Fig. 7(c) shows observed rotor flux waveforms by sliding mode flux observer.

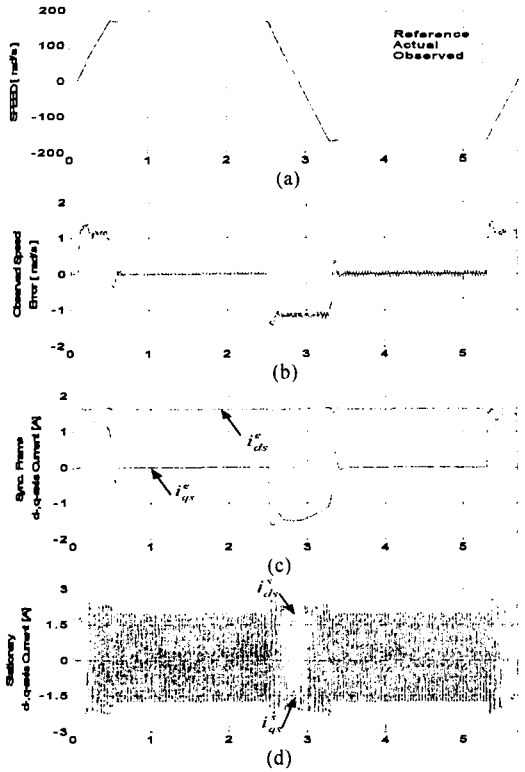

Fig. 5 Simulation result. (a) rotor speed (b) observed speed error (c) d- , q-axis current at sync. Frame (d) stator current

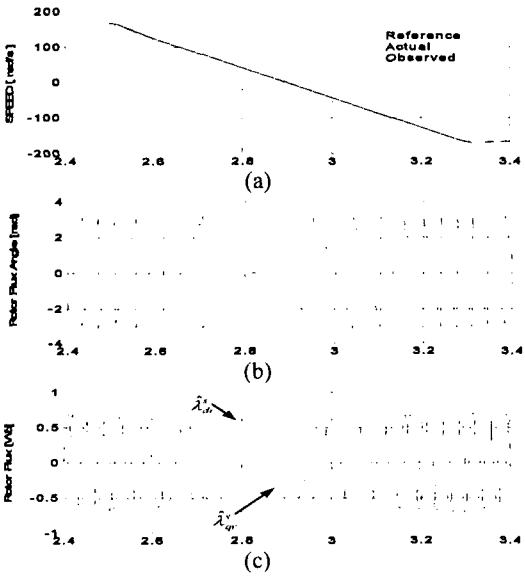

Fig. 6 Simulation result. (a) speed reversion response (b) rotor flux angle (c) observed Rotor flux

4.3. Experimental Results

Experiment for the target system in the paper was achieved in the same process as computer simulation, i.e., at trapezoidal reference(0 [rad/s] → 167.6 [rad/s] → -167.6 [rad/s], ramp rate: 41.9rad/0.1sec) under no load. Because the restriction of implemented inverter rating, maximum exciting current of motor was restricted to 32% of rating. Fig. 7-10 show the experimental response under given condition.

Fig. 7 shows response of trapezoidal speed reference including start-up and speed reversion operation. The dynamic performance of the proposed observer and the experimental

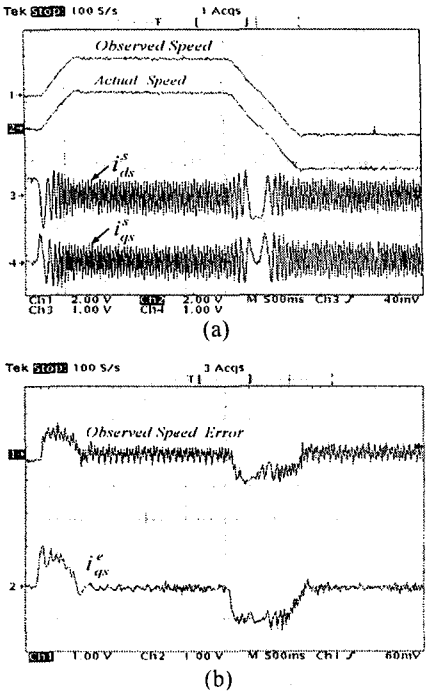

Fig. 7 Trapezoidal reference response (no load)
(a) Speed response and stator current(1A/1V)
(b) Observed speed error(3rad/1V) and Iqse(0.5A/1V)

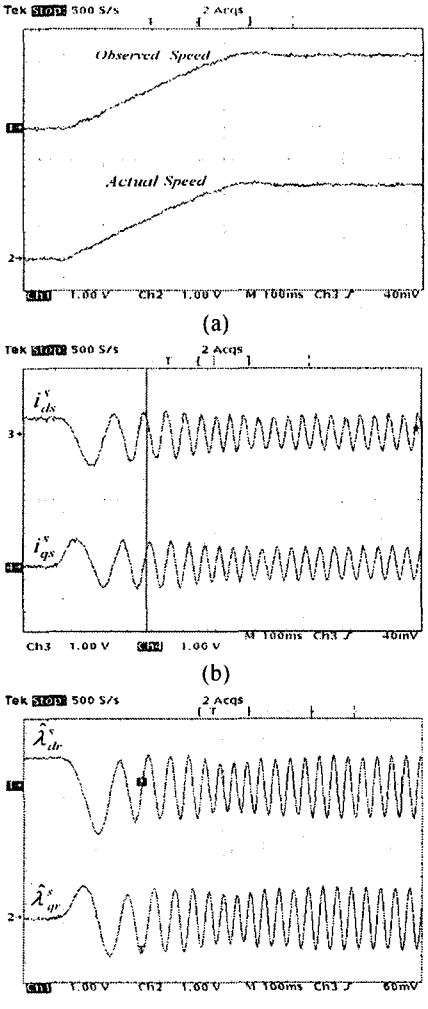

Fig. 8 Start-up response (no load) (a) speed response, (b) stator current(1A/1V), (c) observed rotor flux

IFOC system are satisfactory under the whole operation range, as presented in Fig. 7(b).

Fig. 8 shows the responses at start-up operation. One can notice the capability to maintain the rotor flux/speed estimation by proposed sliding mode observer at standstill.

Fig. 9 and Fig. 10 show responses at the speed reversion. These waveforms demonstrate the speed transition that was achieved smoothly without any transient also at the speed range including zero speed.

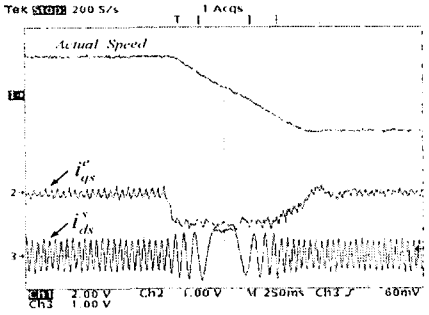

(a)

(b)

Fig. 9 Speed reversion (no load)
(a) Actual speed, Iqse(0.5A/1V), stator current(1A/1V)
(b) Observed rotor flux and position

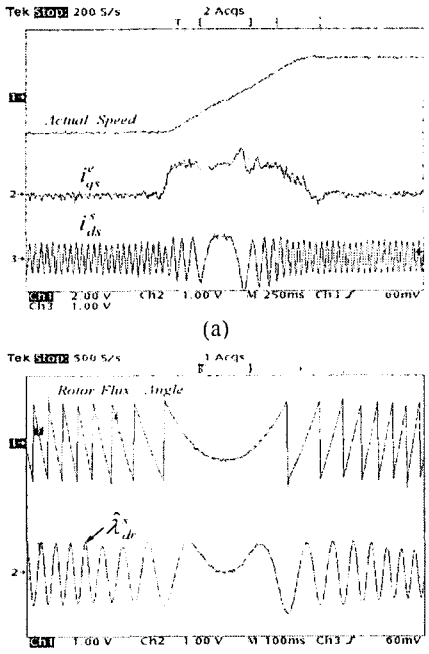

(a)

(b)

Fig. 10 Speed reversion (no load)
(a) Actual speed, Iqse(0.5A/1V), stator current(1A/1V)
(b) Observed rotor flux and position

5. CONCLUSION

A sliding mode flux/speed observer that provides rotor speed estimate for sensorless IFOC of a two-phase induction motor has been presented. Error analysis of the observer has been performed, which shows that the asymptotic stability of the observer can be achieved for any time-varying speed. The computer simulation and experiments was carried out for the speed adjustable sensorless IFOC of 150W two-phase induction motor.The validity and performance of the proposed system was proved by simulation and experimental results.

Though the problem lies in generally high cost compared to fixed- or conventional adjustable speed drive for low power applications, the proposed speed sensorless drive has a great advantage in energy efficiency and relatively low-cost compared to sensored speed vector drive.

References

[1] M. Chomat, T. A. Lipo, "Adjustable-speed single-phase IM drive with reduced number of switches", IEEE Trans. Or Ind. Appl. Vol. 39, No. 3, 2003, pp. 819-825.

[2] D. H. Jang, D. Y. Yoon, "Space-vector PWM technique for two-phase inverter-fed two-phase induction motor", IEEE Trans. On Ind. Appl. Vol. 39, No. 2, 2003, pp. 542-549.

[3] M. Schroedl, "Sensorless control of AC machines at low speed and standstill based on the "INFORM" method" in Conf. Red. IEEE-IAS Annu. Meeting, Vol. 1, 1996, pp 270-277.

[4] P. L. Jansen, R. P. Lorenz, "Transducerless position and velocity estimation in induction and salient AC machines" EEE Trans. Ind. Applicat., vol. 31, pp. 240-247, Mar./Apr. 1995.

[5] H.Kubota, K.Matuse, T. Nakano,"DSP-based speed adaptive flux observer of induction motor", IEEE Trans. Ind. Appl icat., vol. 29, pp. 344-348, Mar./Apr. 1993.

[6] P. Vas, Artificial-Intelligence-based Electrical Machines and Drives – Application of Fuzzy, Neural, Fuzzy-Neural and Genetic-Algorithm-based Techniques. Oxford. U.K.:Oxford Univ. Press, 1999.

[7] V. I. Utkin, Sliding modes in control and optimization. Springer Verlag, 1992.

[8] Zang Yan, Changxi Jin, V. I. Utkin, "Sensorless sliding-mode control of induction motors", IEEE Trans. On Ind. Elec. Vol. 47, No. 6, 2000. pp. 1286-1297.

[9] J. E. Slotine and W. Li. Applied Nonlinear Control. Englewood Cliffs, NJ: Prentice-Hall, 1991.

[10] C. B. Jacobina, M. B. D. R. Correa, E. R. C. D. Silva, A M. N. Lima, "Induction motor drive system for low-power application", IEEE Trans. On Ind. Appl. Vol. 35, No. 1, 1999. pp. 52-61.